



**HAL**  
open science

# Reflux condensation in narrow rectangular channels with perforated fins

Nadia Souidi, André Bontemps

► **To cite this version:**

Nadia Souidi, André Bontemps. Reflux condensation in narrow rectangular channels with perforated fins. *Applied Thermal Engineering*, 2003, 23, pp.871-891. 10.1016/S1359-4311(03)00021-8. hal-00184135

**HAL Id: hal-00184135**

**<https://hal.science/hal-00184135>**

Submitted on 19 Feb 2020

**HAL** is a multi-disciplinary open access archive for the deposit and dissemination of scientific research documents, whether they are published or not. The documents may come from teaching and research institutions in France or abroad, or from public or private research centers.

L'archive ouverte pluridisciplinaire **HAL**, est destinée au dépôt et à la diffusion de documents scientifiques de niveau recherche, publiés ou non, émanant des établissements d'enseignement et de recherche français ou étrangers, des laboratoires publics ou privés.

# Reflux condensation in narrow rectangular channels with perforated fins

N. Souidi <sup>a</sup>, A. Bontemps <sup>b,\*</sup>

<sup>a</sup> GRETh-CEA Grenoble, 17 Rue des Martyrs, 38054 Grenoble Cedex 9, France

<sup>b</sup> LEGI-GRETh, Université Joseph Fourier, 17 Rue des Martyrs, 38054 Grenoble Cedex 9, France

Reflux condensation is an industrial process that aims to reduce the content of the less volatile component or to eliminate the non-condensable phase of a vapour mixture, by the means of separation. Separation consists in condensing the less volatile phase and to recover the condensate while simultaneously, the non-condensable species are recuperated at the top of the system. Compact plate-fin heat exchangers can be used in gas separation processes. The aim of this study is to test the process of reflux condensation of an air–steam mixture in the channels of a plate fin heat exchanger with a hydraulic diameter of 1.63 mm. The experimental study shows that reflux condensation occurs in specific parts of the heat exchanger, the other parts remaining dry.

Moist air condensation is modelled by the film theory and the results show that the model is well adapted to simulating the heat and mass transfer.

*Keywords:* Reflux condensation; Flooding; Rectangular channels; Compact heat exchangers; Heat and mass transfer

## 1. Introduction

The phenomenon of reflux condensation is involved in the chemical, pharmaceutical and oil industries. The principal application of a reflux condenser is to separate the less volatile component from the other species in a mixture of vapours. The reflux condenser has three particular interests compared to a traditional condenser:

---

\* Corresponding author. Tel.: +33-4-76-88-31-55; fax: +33-4-76-88-51-72.  
*E-mail address:* andre.bontemps@cea.fr (A. Bontemps).

## Nomenclature

$a, b$	dimensions of channels [m]
$a$	thermal diffusivity [ $\text{m}^2 \text{s}^{-1}$ ]
$A$	heat transfer area [ $\text{m}^2$ ]
$c_P$	specific heat [ $\text{J kg}^{-1} \text{K}^{-1}$ ]
$C_\tau$	non-dimensional parameter [ ]
$D$	molecular diffusion coefficient [ $\text{m}^2 \text{s}^{-1}$ ]
$D_h$	hydraulic diameter [m]
$g$	acceleration due to gravity [ $\text{m s}^{-2}$ ]
$H$	length [m]
$h$	specific enthalpy [ $\text{J kg}^{-1}$ ]
$\Delta h$	latent heat [ $\text{J kg}^{-1}$ ]
$J$	superficial velocity [ $\text{m s}^{-1}$ ]
$J^*$	dimensionless superficial velocity [ ]
$K$	constant [ ]
$l$	boundary layer thickness [m]
$L$	length [m]
$\dot{m}$	mass velocity [ $\text{kg s}^{-1} \text{m}^2$ ]
$\dot{M}$	mass flow rate [ $\text{kg s}^{-1}$ ]
$n$	number of channels [ ]
$\dot{n}$	molar flow rate per unit area [ $\text{mol m}^{-2} \text{s}^{-1}$ ]
$\dot{N}$	molar flow rate [ $\text{mol s}^{-1}$ ]
$Nu$	Nusselt number [ ]
$O$	origin [ ]
$P$	pressure [bar]
$Pr$	Prandtl number [ ]
$\dot{Q}$	volume flow rate [ $\text{m}^3 \text{h}^{-1}$ , $\text{l h}^{-1}$ ]
$\dot{Q}$	heat flow rate [W]
$\dot{q}$	heat flux [ $\text{W m}^{-2}$ ]
$R_w$	thermal resistance [ $\text{m}^2 \text{K W}^{-1}$ ]
$r$	radial component [m]
$Re$	specific Reynolds number [ ]
$S$	cross sectional area [ $\text{m}^2$ ]
$Sc$	Schmidt number [ ]
$St$	Stanton number [ ]
$t$	time [s]
$T$	temperature [ $^\circ\text{C}$ ]
$u$	axial velocity component [ $\text{m s}^{-1}$ ]
$v$	radial velocity component [ $\text{m s}^{-1}$ ]
$V$	volume [ $\text{m}^3$ ]
$x$	gas mass fraction [ ]

$y$  vapour mass fraction [ ]  
 $z$  axial coordinate [m]

*Greek symbols*

$\alpha$  heat transfer coefficient [ $\text{W m}^{-2} \text{K}^{-1}$ ]  
 $\alpha^*$  corrected heat transfer coefficient [ $\text{W m}^{-2} \text{K}^{-1}$ ]  
 $\beta$  mass transfer coefficient [ $\text{m s}^{-1}$ ]  
 $\beta^{**}$  corrected mass transfer coefficient [ $\text{m s}^{-1}$ ]  
 $\delta$  condensate film thickness [m]  
 $\varepsilon$  dimensionless heat flux [ ]  
 $\eta$  fin efficiency [ ]  
 $\psi$  dimensionless mass flux [ ]  
 $\Gamma$  volume flow rate per wetted perimeter unit [ $\text{m}^2 \text{s}^{-1}$ ]  
 $\lambda$  thermal conductivity [ $\text{W m}^{-1} \text{K}^{-1}$ ]  
 $\mu$  dynamic viscosity [Pa s]  
 $\rho$  mass density [ $\text{kg m}^{-3}$ ]  
 $\tau$  shear stress [ $\text{kg m}^{-1} \text{s}^{-2}$ ]  
 $\xi$  non-dimensional length [ ]  
 $\zeta$  non-dimensional length [ ]

*Indices and superscripts*

d diffusion  
G gas  
i interface  
I incondensable phase  
 $k$   $k$  component  $k = G, L$   
l latent  
L liquid  
ma mass  
M mixture  
R refrigerant  
s sensible  
sat saturation  
t thermal  
 $\tau$  shear stress  
V vapour  
w wall  
 $w_L$  wall side wetted by condensate  
 $w_R$  wall side wetted by coolant  
 $\sim$  molar  
 $\infty$  fully developed regime  
 $-$  average  
[ ] dimensionless

- It can operate as both a heat transfer and a separation device in one.
- Piping requirements are minimised, since units can be mounted directly on top of a distillation column.
- Reflux condensation is a thermodynamically efficient heat and mass transfer process since less heat must be removed to achieve a given separation.

Reducing the heat transfer surface of the heat exchanger by improving its compactness tends to reduce its cost. Compact heat exchangers are currently used in cryogenic gas separation processes where energy consumption is of paramount importance. However, since the process of reflux condensation and the sizing of the units is of such a complex nature, the study of reflux condensation in compact heat exchangers has been neglected. For these reasons both experimental and theoretical work has been carried out to study this phenomenon in a compact geometry.

The expression “reflux condensation” refers to the condensation of a vapour flowing counter-current to its condensate. A reflux condenser aims to separate the various components of a mixture and to recover the condensate at the lower part of the condenser, in some industrial processes, the relevant devices in different sectors being, Webb [1]:

- *Reflux condenser*: heat exchanger in which the gas mixture consists of condensable vapour. The extracted vapour is richer in the most volatile species.
- *Vent condenser*: device intended to reduce as much as possible the incondensable phase of a gas mixture.
- *Dephlegmator*: term equivalent to reflux condenser but used mainly in cryogenics.

This work aims to study reflux condensation flow in a compact heat exchanger with rectangular channels of small characteristic dimensions (hydraulic diameter of 1.63 mm). The motivation for this work is not only to understand and model the physical phenomena (heat and mass transfer), but also to undertake a local rather than a global study of an experimental installation defined and designed according to specific objectives. The literature is poor on studies concerning reflux condensation in mini-channels.

Bakke [2] gives a review of processes where reflux condensers are used to separate mixtures. In his experimental work, he only studied tubes with relatively large diameters and he developed a numerical model of a reflux condenser for binary mixtures.

Jibb et al. [3] highlighted that the film method shows the best agreement with experimental data of reflux condensation in vertical tubes.

Tung et al. [4] proposed a model based on the film theory to describe fractionating condensation in plate-fin devices.

Chen et al. [5] developed correlations for local and average Nusselt numbers for reflux condensation in vertical tubes. These correlations incorporate the effect of interfacial shear stress on the condensate film. However, the minimum tube diameter for which the correlations are still valid is not given.

For the case of reflux condensation of moist air in narrow rectangular channels with perforations, no results are available.

## 2. Simulation of reflux condensation

The film theory, initially developed by Colburn and Hougen [6], is established on the assumption that a one-dimensional gas layer or film adjacent to the interface between the liquid and gas phases exists. The resultant temperature profiles are shown in Fig. 1. The partial pressure is related to the concentration and the temperature varies from the bulk to the interface as represented in Fig. 1.

The film is supposed laminar and transfers occur by mass diffusion and heat conduction. The principle of modelling is established on the existence of two distinct and coupled flows: the axial counter-current liquid–gas flow and the radial heat and mass transfers. The radial heat and mass transfers take place in the film in the vicinity of the interface and are directional according to an  $Or$  axis whose origin is located in the gas mixture bulk. The counter-current flow is orientated following the  $Oz$  axis whose origin is located at the vapour entrance. The flow is divided into four zones, as indicated in Fig. 1. The usual assumptions will be done in establishing the following relations.

### 2.1. Heat and mass transfer

The molar flux of the vapour  $\dot{n}$  divides up into transported and diffusional components [7]:

$$\dot{n} = \tilde{y}_V \dot{n} - \tilde{\rho}_M D_{VG} \frac{d\tilde{y}_V}{dr}, \quad (1)$$

where  $\tilde{y}_V$  is the mole fraction of the vapour,  $\tilde{\rho}_M$  the total molar concentration and  $D_{VG}$  the molecular diffusion coefficient.

Taking into account the hypotheses of the theory, the following expression of the molar flux is obtained:

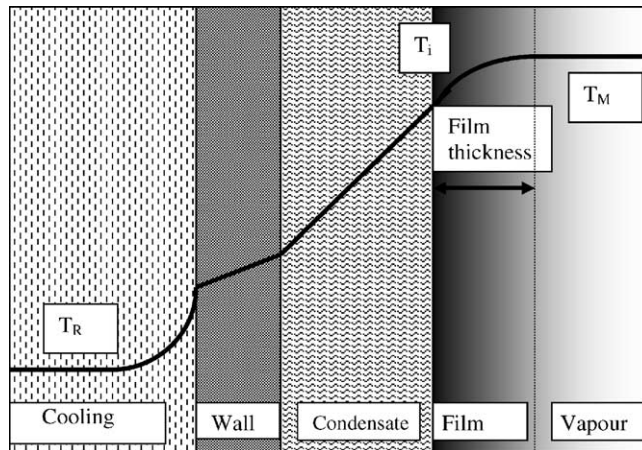


Fig. 1. Temperature evolution in an incondensable-vapour mixture.

$$\dot{n} = \tilde{\rho}_M \beta_V \ln \left\{ \frac{1 - \tilde{y}_{Vi}}{1 - \tilde{y}_{VM}} \right\}, \quad (2)$$

where  $\beta_V$  is the mass transfer coefficient.

Sometimes, by analogy with heat transfer, a corrected mass transfer coefficient  $\beta_V^{**}$  is defined as

$$\beta_V^{**} = \beta_V \frac{1}{\tilde{y}_{VM} - \tilde{y}_{Vi}} \ln \left\{ \frac{1 - \tilde{y}_{Vi}}{1 - \tilde{y}_{VM}} \right\} \quad (3)$$

and the molar flux can be written:

$$\dot{n} = \beta_V^{**} \tilde{\rho} (\tilde{y}_{VM} - \tilde{y}_{Vi}). \quad (4)$$

The heat flow exchanged in the system is the contribution of a latent heat flow and a sensible and convective heat flow. In the case of a vapour mixture and non-condensable gas, the latent heat flux is reduced to the expression:

$$\dot{q}_l = \dot{n} \Delta \tilde{h}_{LV}, \quad (5)$$

$\Delta h_{LV}$  being the latent heat.

The combined sensible and conductive fluxes to the interface are:

$$\dot{q}_s = \dot{n} \tilde{c}_{pV} (T - T_i) - \lambda_V \frac{dT}{dr}. \quad (6)$$

The heat flow exchanged in the system is the contribution of the conductive and convective heat flux as calculated above and of the latent heat flux. Introducing the non-dimensional parameter  $\varepsilon = ((\dot{n} c_{pV}) / \alpha_V)$ , where  $\alpha_V$  is the gas-phase heat transfer coefficient, the total heat flux is thus written in the following way:

$$\dot{q} = \alpha_V \frac{e \exp(\varepsilon)}{\exp(\varepsilon) - 1} (T_M - T_i) + \dot{n} \Delta \tilde{h}_{LV}. \quad (7)$$

The composition of vapour at the interface is related to the saturated vapour pressure by the following equation:

$$y_i = \frac{P_i}{P} = \frac{P_{\text{sat}}(T_i)}{P}. \quad (8)$$

Defining the heat flux between the gas mixture bulk and the interface by:

$$\dot{q} = \alpha_V^* (T_M - T_i) + \Delta \tilde{h}_{LV} \dot{n} \quad (9)$$

with

$$\alpha_V^* = \alpha_V \frac{\varepsilon \exp(\varepsilon)}{\exp(\varepsilon) - 1} \quad (10)$$

and the heat flux between the interface and the coolant by

$$\dot{q}_L = \alpha_L (T_i - T_{wL}) = \frac{1}{R_w} = \alpha_R (T_{wR} - T_R), \quad (11)$$

it is possible to write the energy balance at the interface. In Eq. (11),  $T_{wL}$  and  $T_{wR}$  are the wall temperatures on the condensate side and on the coolant side respectively. Heat transfer areas can be very different since they are finned surfaces (Fig. 3). It is thus necessary to express the energy balance in terms of heat flow rates in the form

$$\dot{Q} = \dot{Q}_L \quad (12)$$

with

$$\dot{Q} = A_M[\eta_M\alpha_V^*(T_M - T_i) + \Delta\tilde{h}_{LV}\dot{n}], \quad (13)$$

where  $A_M$  is the heat transfer surface area wetted by the condensate and  $\eta_M$  is the efficiency of finned surface and

$$\dot{Q}_L = A_M\alpha_L(T_i - T_{wL}) = A_R\eta_R\alpha_R(T_{wR} - T_R), \quad (14)$$

where  $A_R$  is the heat transfer surface area wetted by the cooling water and  $\eta_R$  is the efficiency of the cooling side finned surface.

## 2.2. Counter-current flow simulation

### 2.2.1. Mass balances

The main variables used as well as the flow directions are represented in Fig. 2. Considering the surface element  $dA = (a + b) dz$ , (Fig. 3), the decrease  $d\dot{N}$  in the total number of moles of gas is the same as the number of moles that are transferred in the liquid film formed by the condensate,  $\dot{n}_L dA$ . The cross section of the formed condensate flow is  $S_L$ .

The balance on the control volume defined by  $S_L dA$  gives the following equation.

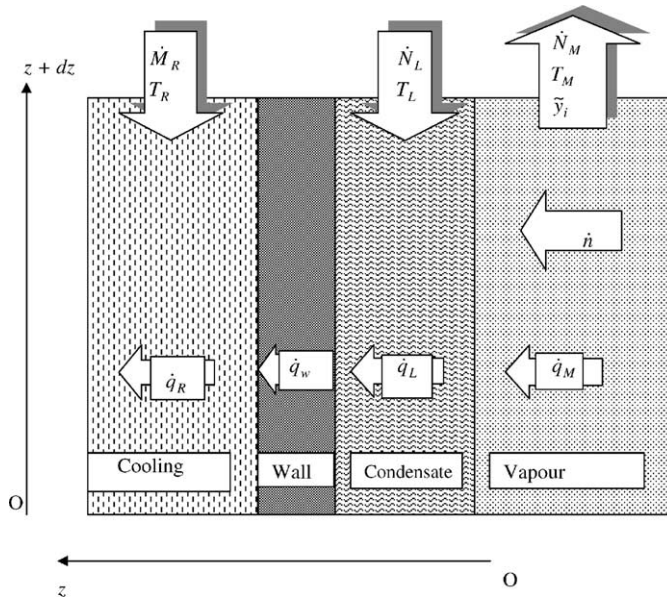


Fig. 2. Schematic view of the modelled system and flow directions.

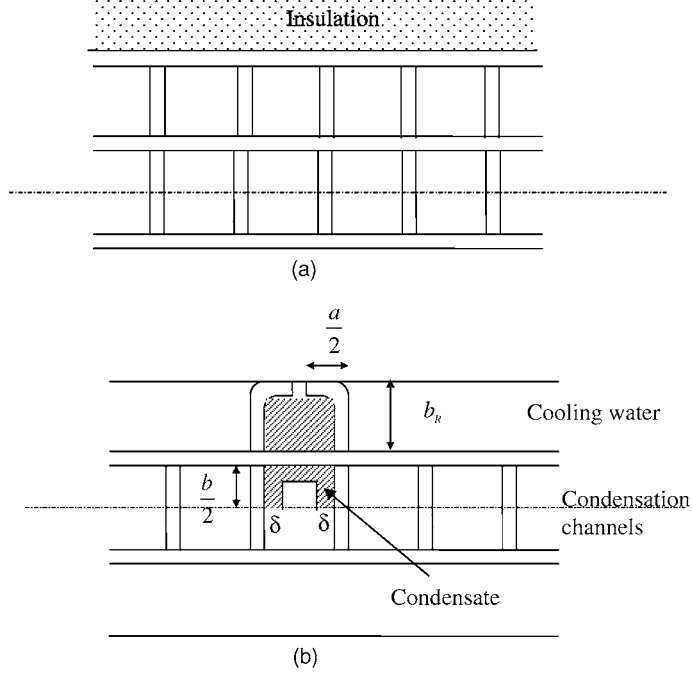


Fig. 3. Cross section of the condenser and chosen geometrical model, (a) coolant side and condensation side channel, (b) adopted geometrical model: definition of fins on the cooling water side.

*In the liquid phase:*

$$\frac{\partial \dot{N}_L}{\partial z} = (a + b)\dot{n}_L. \quad (15)$$

*In the vapour phase:*

$$\frac{\partial \dot{N}_V}{\partial z} = -(a + b)\dot{n}_V. \quad (16)$$

*In the incondensable phase and in the coolant:*

$$\frac{d\dot{N}_I}{dz} = 0 \quad \text{and} \quad \frac{d\dot{N}_R}{dz} = 0. \quad (17)$$

### 2.2.2. Heat balance

In the gas phase, if  $\tilde{h}_M$  is the molar enthalpy of the mixture at the temperature  $T_M$ , and if  $\tilde{h}_{Li}$  is the molar enthalpy at the interface temperature  $T_i$ , the enthalpy balance on the vapour mixture in the control volume  $S_V dz$  is:

$$\frac{d(\dot{N}_M \tilde{h})}{dA} = -\dot{n}_M \tilde{h}_{Li} - \dot{q}_M \quad (18)$$

or

$$\dot{N}_M \tilde{c}_{PM} \frac{dT_M}{dA} = \dot{n}_M \tilde{c}_{PM} (T_M - T_i) - \dot{q}_M \quad \text{with} \quad \dot{q}_M = \alpha_V^* (T_M - T_i). \quad (19)$$

In the coolant,

$$\dot{m}_R c_{PR} dT_R = \alpha_R \eta_R (T_{wR} - T_R) dA_R. \quad (20)$$

In the condensate film,

$$\frac{d(\tilde{h}_L \dot{N}_L)}{dA} = -\dot{q}_w + \dot{n}_M \Delta \tilde{h} Li + \dot{q}_M. \quad (21)$$

### 2.2.3. Momentum balance in the vapour/non-condensable phase

The pressure loss is calculated from the momentum equations. If  $\dot{M}$  is the mass flow rate of the gas, the average mixture velocity is defined by:

$$\bar{u}_M = \frac{\dot{M}}{S_V \rho_M}. \quad (22)$$

If  $\dot{m}$  is the mass flux density and  $\tau_i$  the shear stress at the interface, in a volume element  $dV = S_V dz$  the momentum balance is written as:

$$dP S_V = -\frac{d\dot{M}^2}{\rho_M} \frac{1}{S_V} + \tau_i dS_V - \rho_M g dV \quad (23)$$

which upon introduction of the hydraulic diameter:

$$\frac{dP}{dz} = 2 \frac{\bar{u}_M \dot{m}}{D_h} + 4 \frac{\tau_i}{D_h} - \rho_M g \quad (24)$$

with

$$\tau_i = 0.5 C_\tau \rho_M \bar{u}_M^2. \quad (25)$$

For a rectangular channel Shah and Bhatti [8] proposed:

$$C_\tau = \frac{24}{Re_L} \left( 1 - 1.3553 \frac{a}{b} + 1.9467 \left( \frac{a}{b} \right)^2 - 1.7012 \left( \frac{a}{b} \right)^3 + 0.9564 \left( \frac{a}{b} \right)^4 - 0.2537 \left( \frac{a}{b} \right)^5 \right) \quad (26)$$

in a laminar flow ( $Re < 2300$ ) and

$$C_\tau = 0.079 Re_L^{-1/4} \quad (27)$$

in a turbulent flow.

### 2.2.4. Momentum balance in the condensate film [9]

Considering the diagram of Fig. 4 representing the film flow on a vertical wall, with the help of the usual assumptions, the system of equations describing the balance of a laminar fluid section is the following:

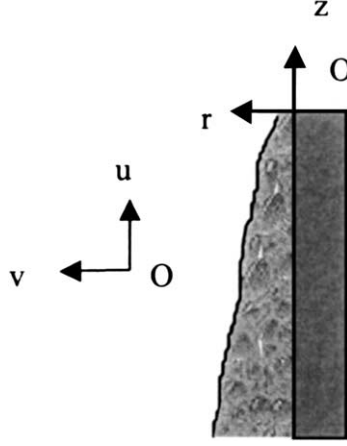


Fig. 4. Flow characteristics on the wall.

$$\begin{cases} \rho_L \left( u \frac{\partial u}{\partial z} + v \frac{\partial u}{\partial r} \right) = -\frac{\partial P}{\partial z} + \mu_L \left( \frac{\partial^2 u}{\partial r^2} + \frac{\partial^2 u}{\partial z^2} \right) - \rho_L g, \\ \frac{\partial u}{\partial z} + \frac{\partial v}{\partial r} = 0, \end{cases} \quad (28)$$

$r$  being of the magnitude of the condensate film thickness  $\delta$  and  $z$  being of the order of the height  $H$ . Given that  $\delta \ll H$ , the variations following  $z$  are weak compared to those following  $r$ , thus:

$$-\frac{\partial P}{\partial z} + \mu_L \frac{\partial^2 u}{\partial r^2} - \rho_L g = 0. \quad (29)$$

At the interface, the friction between the gas and the condensate is given by the shear stress:

$$\tau_i = \mu_L \left. \frac{du}{dr} \right|_{r=\delta}. \quad (30)$$

The velocity distribution in the condensate as a function of the film thickness is obtained:

$$u = \frac{1}{\mu_L} \left[ \left( \rho_L g + \frac{dP}{dz} \right) \left( \frac{r^2}{2} - \delta r \right) + \tau_i r \right]. \quad (31)$$

The mass flow rate is calculated using the condensate average velocity:

$$\bar{u} = \frac{1}{\delta} \int_0^\delta u(r) dr \quad (32)$$

and

$$\bar{u} = -\frac{1}{\mu_L} \left[ \left( \rho_L g + \frac{dP}{dz} \right) \frac{\delta^2}{3} - \frac{\tau_i \delta}{2} \right]. \quad (33)$$

The mass flow per unit of perimeter is defined by

$$\Gamma = \int_0^\delta \rho_L u dy = \rho_L \delta \bar{u} \quad (34)$$

and is given by:

$$\Gamma = \frac{\rho_L}{\mu_L} \left[ - \left( \rho_L g + \frac{dP}{dz} \right) \frac{\delta^3}{3} + \frac{\tau_i \delta^2}{2} \right] \quad (35)$$

and the mass flow rate is thus written:

$$\dot{M} = L\Gamma, \quad (36)$$

$L$  being the characteristic length:

$$L = a + b. \quad (37)$$

### 2.3. Evaluation of heat and mass transfer coefficients

The mass transfer coefficient is determined using the Chilton-Colburn [10] analogy:

$$\beta_V = \left( \frac{\alpha_V}{\rho_V c_P} \right) \left( \frac{Pr_V}{Sc_V} \right)^{2/3}. \quad (38)$$

The local heat transfer coefficient in the vapour is evaluated as proposed by the formula of Shah and Bhatti [8] for a rectangular channel:

$$Nu_V(z) = Nu_\infty + \frac{0.024z^{*-1.14}(0.0179Pr_V^{0.17}z^{*-0.64} - 0.14)}{(1 + 0.0358Pr_V^{0.17}z^{*-0.64})^2}, \quad (39)$$

where

$$z^* = \frac{z}{D_h Re_V Pr_V} \quad (40)$$

and  $Nu_\infty$  is the value of the Nusselt number for a fully developed flow:

$$\overline{Nu}_\infty = 7.541 \left( 1 - 2.61 \frac{a}{b} + 4.97 \left( \frac{a}{b} \right)^2 - 5.119 \left( \frac{a}{b} \right)^3 + 2.702 \left( \frac{a}{b} \right)^4 - 0.548 \left( \frac{a}{b} \right)^5 \right), \quad (41)$$

$a$  and  $b$  being the channel dimensions.

In our case:

$$\overline{Nu}_\infty = 5.06. \quad (42)$$

The heat transfer coefficient in the condensate is evaluated as proposed by Chen et al. [5] with the use of the Boyko and Krushilin [11] correlation:

$$Nu = \left( \frac{D_h}{\lambda_L} \right) \alpha_L \left( 1 + y \left( \frac{\rho_L}{\rho_V} - 1 \right) \right)^{1/2}. \quad (43)$$



Table 1  
Fin characteristics of the test section

Fins characteristics	Length (mm)	Height (mm)	Gap (mm)	Thickness (mm)	Hydraulic diameter (mm)
Perforated (5%)	400	6.93	1.21	0.2	1.63

culates in ten passes from the top to the bottom of the test section. The mixture enters the central channel at the lower end of the test section. The lateral and the central channels are made of plates with plain and perforated fins respectively (Table 1 and Fig. 6). The temperatures are measured by means of K type thermocouples. The steam–air mixture temperatures are measured with 4 thermocouples inside the test section (Fig. 6) and 2 thermocouples at the inlet and the outlet. The

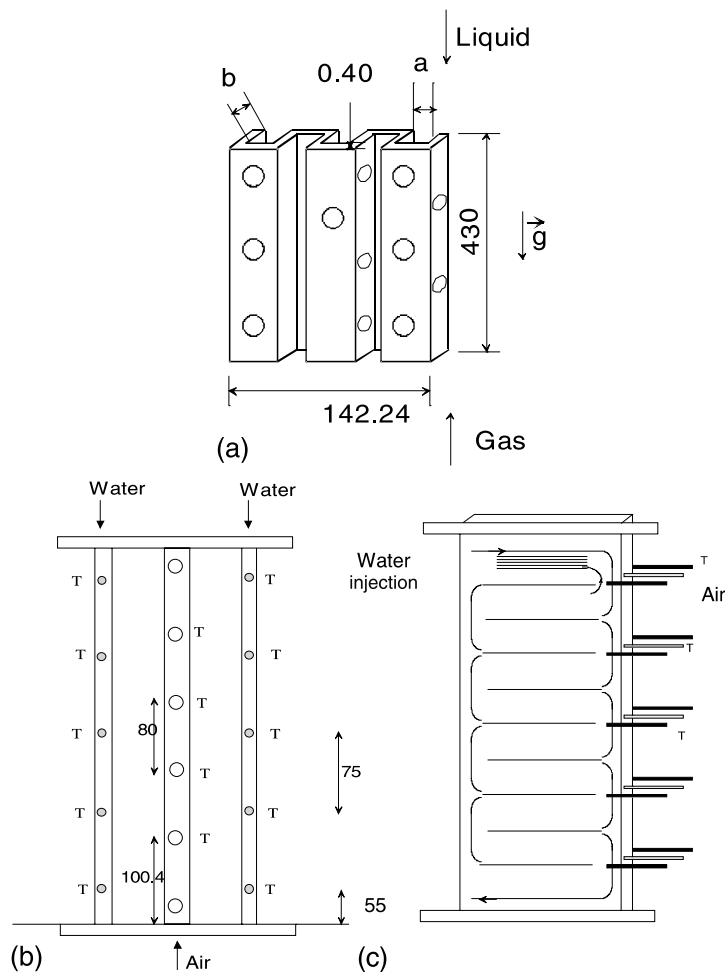


Fig. 6. Characteristics of the test section, (a) fin characteristics, (b) instrumentation, (c) cooling system. Dimensions are given in millimeters. T is for thermocouple.

cooling temperatures are measured by 10 thermocouples located between each pass plus 2 thermocouples at the inlet and outlet.

### 3.3. Vapour and condensate circuit

The steam–air mixture produced in the boiler enters the test section and the steam partly condenses. The air and the non-condensed steam escape higher to a final condenser designed to complete the process. The condensate falls down via gravity. Its flow rate is then evaluated in the measurement container. The air is rejected to the atmosphere.

### 3.4. Coolant circuit

This circuit allows the water flow rate and temperature to be controlled. This includes three rotameters to measure the water flow rate, and a cooler.

### 3.5. Experimental procedure and data reduction

The flow rate of the cooling water is first regulated and then the air flow rate is adjusted together with the heating wire. The rheostat is adjusted to regulate the power of the boiler and the acquisition system is initiated.

The measurements of the cooling water flow rate and the temperatures at the entrance and at the exit of the test section give the total heat flux on the cooling water side:

$$\dot{Q}_R = \dot{m}_R c_{PR} \Delta T_R. \quad (44)$$

Here  $\Delta T_R$  is the temperature difference between the entrance and the exit of the cooling water in the test section.

The circuit being well insulated, it is assumed that the heat transferred to the cooling water corresponds to  $\dot{Q}$ , the heat released by the mixture.

## 4. Results

### 4.1. Experimental results

#### 4.1.1. Temperatures in cooling water and in moist-air

Figs. 7 and 8 represent the temperature profiles of cooling water and moist-air respectively as a function of the height  $z$  of the condenser. Measurements were carried out using the thermocouples directly introduced into the fluid (water) or in the central condensation channel containing moist air. Qualitatively, three types of profile were observed as a function of the flow of cooling water entering the test section (Fig. 9):

1. In the first case, the temperature decreases gradually and tends towards an asymptote at the higher part of the condenser. This type of profile is observed for the higher cooling water flow rates (40–60 l h<sup>-1</sup>).

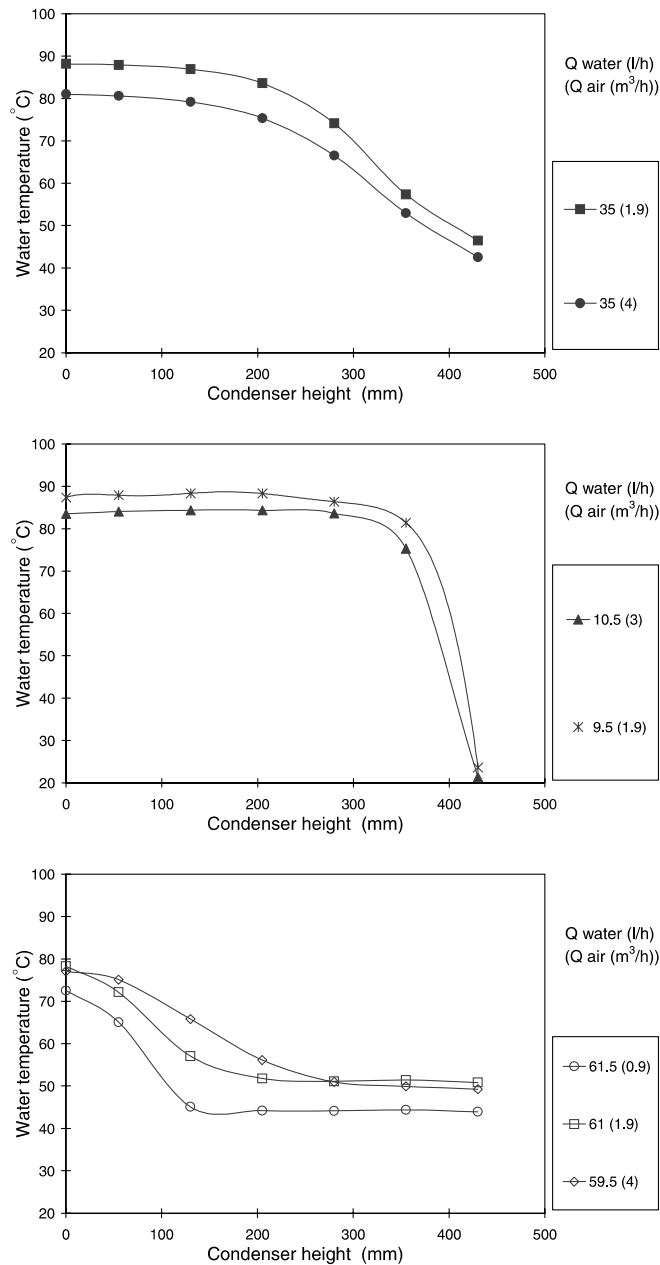


Fig. 7. Temperature evolution in the cooling water.

2. The profile observed is more uniform since the temperature decreases uniformly along the heat exchanger. This corresponds to medium flow rate of cooling water (30–40  $l\ h^{-1}$ ).
3. In this third configuration, the temperature remains practically constant in the lower part of the heat exchanger only to drop abruptly in the higher part. The flow rate of cooling water is then rather low (10–20  $l\ h^{-1}$ ).

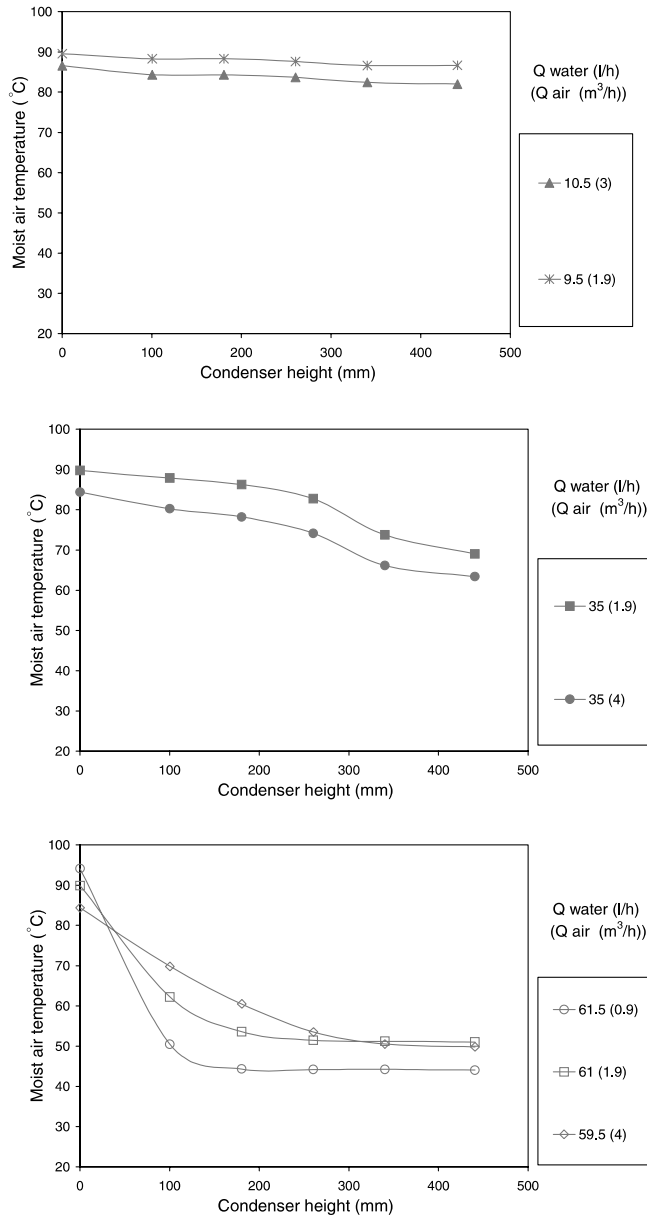


Fig. 8. Temperature evolution in the mixture.

#### 4.1.2. Evolution of the condensation process

The air molar fraction evolution as a function of various flow rates of cooling water is represented on Fig. 9 together with cooling powers. In the case of the high flow rate, it is clearly shown that the molar fraction profile increases only in the lower part of the heat exchanger. For

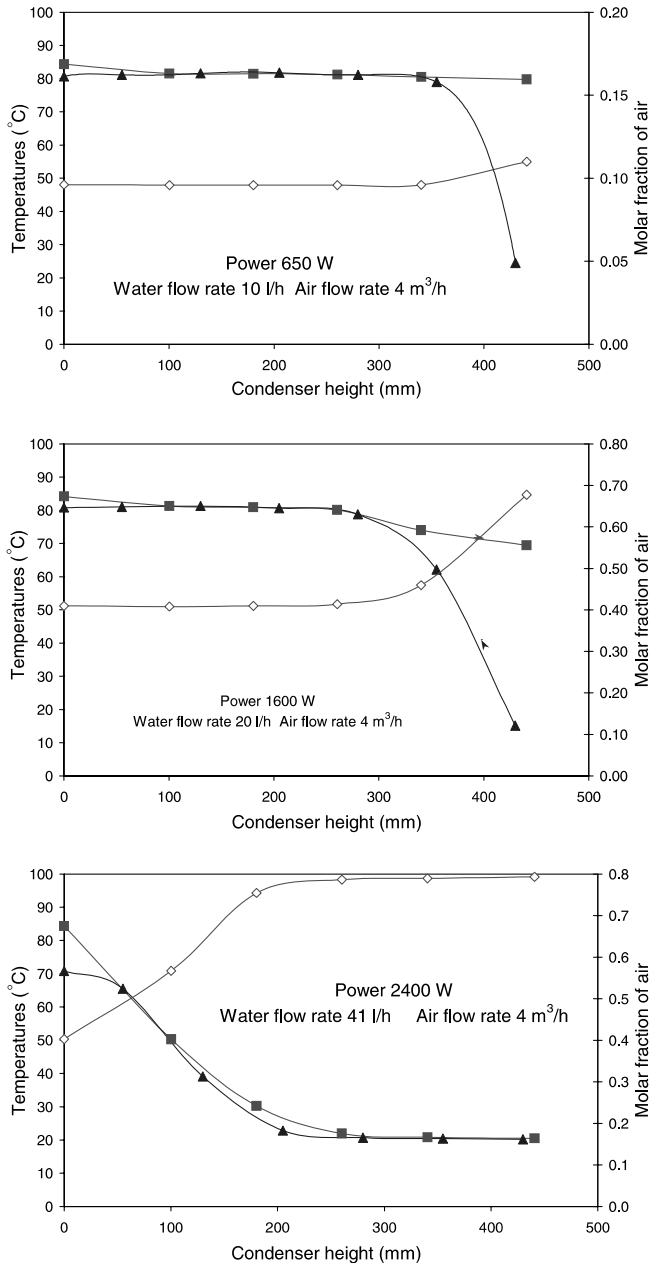


Fig. 9. Experimental results: (□) air molar fraction, (△) cooling water temperature, (◆) moist air temperature.

low flow rates, the molar fraction evolves only along the higher part. For the two previous flow rates, the heat exchanger does not operate in normal conditions. On the contrary, for the medium flow rates, the heat exchanger is working along its total length.

#### 4.1.3. Discussion

The two preceding paragraphs underline the importance of two parameters for the experimental results: the temperatures and the composition of the mixture. Temperatures and the composition of the mixture are now examined together to validate the observations.

Figs. 7 and 8 represent each profile of water and moist air temperature in cases of increasing cooling powers, for two distinct air flow rates, 1 and 4 m<sup>3</sup> h<sup>-1</sup>. On each figure, using a scale of the Y-axis, the evolution of the molar composition of the air along the condenser is represented. The following phenomena are observed:

- For high exchanged powers (>2000 W), the temperatures and the compositions tend towards an asymptotic value in the higher part of the condenser. This phenomenon indicates that most of the cooling and thus condensation are achieved on the lower part of the condenser.
- For medium exchanged powers (≈1500 W), condensation occurs all along the test section. The decrease in temperature and composition along the exchanger is regular.
- Finally, for low exchanged powers (<1000 W), condensation takes place at the higher part of the condenser, the temperature profiles being asymptotic in the lower part.

For an air composition at the input of the condenser, the main parameters acting on the phenomenon of condensation are: the exchanged cooling power, the cooling water flow rate (coupled with the preceding parameter), and the inlet temperature of cooling water.

The exchanged power determines the condensate flow rate and is directly related to the flow rate of cooling water. Moreover, when this water flow rate is high, the temperature of the wall is imposed and only varies slightly between the inlet and the outlet.

The water temperature fixes the air concentration after condensation. This is particularly clearly marked when comparing the curves corresponding to inlet temperatures of the water of 50 °C (flow rate of water 62 l h<sup>-1</sup>, exchanged power 2000 W) and 30 °C (water flow rate 51 l h<sup>-1</sup>, exchanged power 2100 W) in Fig. 8, where it is observed that the air compositions are respectively 32% and 70%.

In order to confirm these observations, the evolution of the flow rate of the condensate in the test section and the post-condenser (container C<sub>2</sub>) as a function of the air flow rate (high

Table 2

Comparison of the characteristics of the two test sections used for both condensation and adiabatic experiments

Counter-current air–water experimental study with perforated fins	Moist air condensation in perforated fins
<i>Test section</i>	
Channel dimensions: 5.10 × 2.14 (mm)	Channel dimensions: 6.93 × 1.21 (mm)
Thickness: 0.4 (mm)	Thickness: 0.2 (mm)
Perforation gap: 20 (mm)	Perforation gap: 20 (mm)
Plate dimensions: 142 × 430 (mm <sup>2</sup> )	Plate dimensions: 120 × 400 (mm <sup>2</sup> )
<i>Flow rates</i>	
Water: 5–300 (l h <sup>-1</sup> )	Water (condensate): 0–5 (l h <sup>-1</sup> )
Air: 0–6 (m <sup>3</sup> h <sup>-1</sup> )	Moist air: 0–6 (m <sup>3</sup> h <sup>-1</sup> )

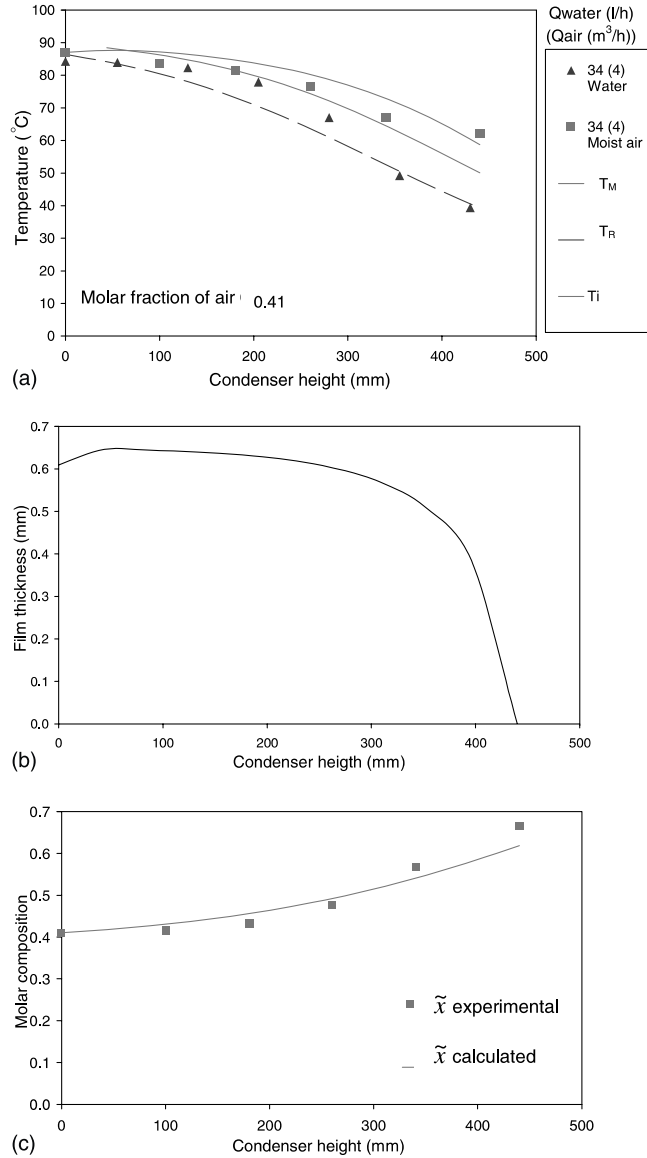


Fig. 10. Comparison of theoretical and experimental results, (a) temperatures profiles, (b) film thickness, (c) composition:  $T_M$  theoretical moist air temperature,  $T_R$  theoretical cooling water temperature,  $T_i$  theoretical gas-liquid interface temperature.

and low water flow rates) is shown in Fig. 8. For the high flow rates, the condensate flow rate in the second condenser is zero. This means that condensation is complete in the test section. For the low cooling water flow rates, the flow rate in the post-condenser is significant. This condenser is used to complete the dehumidification of the air exiting the test section (Table 2).

## 4.2. Theoretical analysis

The graphs in Fig. 10 represent the calculated temperature profiles  $T_R$  and  $T_M$  in the cooling water and in the steam–air mixture respectively along the heat exchanger.

The experimental conditions correspond to a medium exchanged power for which the condensation occurs over the whole heat exchanger. All the results obtained in this case of medium exchanged power are similar to the one presented in this section.

It is noticed that the calculated profiles are similar to the experimental ones with a maximum difference of 7%. The calculated temperature of the liquid gas interface  $T_i$ , is also represented. This last temperature seems to suitably match the temperature of moist air with an error lower than 1%, except for the last value where the error is near 10%. The thermocouples introduced in the moist air channel thus give results closer to the value of the interface temperature than to the bulk gas value. As a consequence, it is probable that the thermocouples are wetted by the condensate. Indeed, in this case, the flow of cooling water is medium ( $35 \text{ l h}^{-1}$ ) and condensation is thus regular and abundant compared to the size of the channel. Fig. 10(b) represents the evolution of the simulated film thickness. This thickness varies from 0.4 to 0.6 mm. For the small thickness, the theoretical value of  $T_i$  is practically identical to the experimental data. Channels dimensions are  $6.93 \times 1.21 \text{ mm}^2$  and, taking into account the communication between the side channels (perforations), this calculated result confirms that the thermocouples are probably regularly flooded by the condensate except for the last point of measurement ( $\approx 64 \text{ }^\circ\text{C}$  for 440 mm). Indeed, at this coordinate of the heat exchanger, the film thickness is very thin and the temperature of the mixture is really measured as indicated by the simulation. Comparison between the theoretical and the experimental profiles of the molar composition of the air (Fig. 10), shows good agreement between the theory and the experiment.

## 5. Conclusion

Reflux condensation of a vapour–air mixture was studied in a compact heat exchanger with rectangular channels of small characteristic dimensions (hydraulic diameter of 1.63 mm). An experimental installation has been designed to carry out a local study of reflux condensation which allow local vapour temperatures to be measured. A theoretical work has been undertaken to model heat and mass transfer when reflux condensation occurs.

The film theory is well adapted to model the condensation of the studied mixture. This method has been adapted to the specific case of reflux condensation in narrow channels. The results shows that the choice of the correlations is adequate.

In the experimental study, three distinct zones of operation are discerned for this type of heat exchanger. The dimensions of the zones depend mainly on the values of the flow rate and the temperature of the cooling water, and consequently on the exchanged heat flow. These parameters help to determine the value of the condensate flow rate and thus, the final composition of the mixture. In such a counter-current heat exchanger, there are preferential regimes of condensation depending on the intensity of the heat flux exchanged.

When comparing the theoretical and experimental results, a fair agreement is found. This agreement becomes excellent when remarking that the measured temperatures can be either the

mixture temperature or the condensate temperature knowing that thermocouples can be wetted or not.

## References

- [1] D.R. Webb, Future needs and developments in heat exchanger technology, in: *Condensation, Heat Exchange Engineering, European Research Meeting-Birmingham*, HEE 96/R1, 1996.
- [2] K. Bakke, Experimental and theoretical study of reflux condensation, Ph.D. Thesis, Norwegian Institute of Science and Technology, 1997.
- [3] R.J. Jibb, I. Gibbard, G.T. Polley, D.R. Webb, The potential for using heat transfer enhancement in vent and reflux condensers, in: *Heat Transfer in Condensation and Evaporation, Eurotherm 62, GRETh*, 1998.
- [4] H.H. Tung, J.F. Davis, R.S.H. Mah, Fractionating condensation and evaporation in plate-fin devices 32 (1986) 1116–1124.
- [5] S.L. Chen, F.M. Gerner, C.L. Tien, General film condensation correlations, *Exp. Heat Transfer* 1 (1987) 93–107.
- [6] A.P. Colburn, O.A. Hougen, Design of cooler condensers for mixtures of vapour with non-condensing gases, *Ind. Eng. Chem.* 26 (1934) 1178–1182.
- [7] R. Taylor, R. Krishna, *Multicomponent Mass Transfer*, John Wiley & Sons, New York, 1993.
- [8] R.K. Shah, M.S. Bhatti, in: S. Kakac, R.K. Shah, W. Aung (Eds.), *Handbook of Single-Phase Convective Heat Transfer*, Wiley-Interscience, New York, 1987 (Chapter 3).
- [9] W. Nusselt, The condensation of steam on cooled surface, *Chem. Eng. Fund.* 1 (1982) 6.
- [10] T.H. Chilton, A.P. Colburn, Mass transfer coefficients: prediction from data on heat transfer and fluid friction, *Ind. Eng. Chem.* 1 (26) (1934) 1183–1187.
- [11] L.D. Boyko, N. Kruzhilin, Heat transfer and hydraulic resistance during condensation of steam in horizontal tube and in a bundle of tubes, *Int. J. Heat Mass Transfer* 10 (1967) 361–373.